

Atomic force microscopy of DNA self-assembled on a highly oriented pyrolytic graphite electrode surface

Xiaohua Jiang, Xiangqin Lin *

Department of Chemistry, University of Science and Technology of China, Hefei 230026, PR China

Received 26 May 2004; received in revised form 18 June 2004; accepted 21 June 2004

Available online 14 July 2004

Abstract

Different types of self-assembled DNA networks were obtained and characterized by tapping mode atomic force microscopy (AFM) on highly oriented pyrolytic graphite (HOPG) electrodes. Both native calf thymus DNA and synthetic DNA with specific base sequences were investigated. The freely adsorption of DNA on the surface of HOPG forms two-dimensional networks. The double-stranded DNA molecules may form cross-linking points on double helix chains, forming intermediate attachments. The differences in AFM morphology of these DNA condensations can be related to the intrinsic properties of the DNA, which lead to different interactions with HOPG. Three-dimensional networks were formed on the HOPG under applied electric field. The effects of external electric field on the condensation of calf thymus DNA have been investigated in detail. It led to a proposition that the DNA molecules may be polarized in the electric field, and attached to the HOPG surface via its one end with the phosphate backbone lying or standing on the substrate depending on the applied potential. The AFM morphological changes of DNA in the presence of external electric field provided insight into DNA interactions.

© 2004 Elsevier B.V. All rights reserved.

Keywords: DNA; Self-assembled networks; Controlled potential; AFM; HOPG

1. Introduction

The molecular self-assembly on solid substrates has been intensely studied for more than 20 years [1]. DNA is one of the most promising molecules for this investigation due to its conformational flexibility, inherent programmability through the sequence and its moderate resistance to degradation [2–5]. Surfaces modified with single- or double-stranded DNAs have been investigated for potential usages in biosensing and biochemical imaging [6–9]. In addition, the electrochemical properties of redox-active intercalators bound to DNA-modified electrodes have been analyzed to probe the charge transport through the extended-stack of the DNA helix [10]. It is

essential to understand the surface structure of these modified electrodes, since different DNA conformation leads to different interactions with small molecules. Moreover, it is important to determine the effect of applied electric field on the DNA surface conformation, since many of the biosensing applications involve electrochemical detection schemes. However, the specific interactions of DNA molecules with electrode surfaces, the conformations of immobilized DNA, and the degree of surface coverage under different conditions are still not very clear, despite of the extensive use of DNA biosensors. The formation of DNA films depends not only on the electrode and DNA characteristics, but also the concentration of DNA and the procedure adopt for immobilization. A better understanding of these factors is necessary for sensor development.

In this paper, tapping mode AFM was used to characterize the surface morphology of a DNA-based

* Corresponding author. Tel.: +86-551-3606646; fax: +86-551-3601592.

E-mail address: zqlin@ustc.edu.cn (X. Lin).

electrochemical biosensor fabricated under different procedures. Native calf thymus DNA and synthetic short DNA were studied. We have observed that a well-defined DNA networks formed on the substrate could undergo dramatic morphological changes as a function of applied electrochemical potential. Possible mechanism for DNA free adsorption and electrochemical deposition on HOPG was proposed.

2. Experiment

2.1. Materials

Native calf thymus double-stranded DNA (23,000 bp, $A_{260}/A_{280} > 1.8$, denoted as CTDNA), 20 bp oligo(dA)·oligo(dT) and 20 bp oligo(dG)·oligo(dC) were all purchased from Sino-American Biotechnical, Co. A pH 7.1 solution of 50 mM NaCl+5 mM Tris-HCl buffer (THB) was prepared for DNA dissolution.

Highly oriented pyrolytic graphite (HOPG, grade ZYH, from NT-MDT Co., Russia) was used as a substrate throughout this study.

2.2. Electrochemical apparatus

Voltammetric experiments were carried out in a one-compartment electrochemical cell. The HOPG sample, as the working electrode, was embedded in a Teflon block and led out by copper wire. A Pt wire counter electrode and an Ag/AgCl wire quasi-reference electrode were used. Electrochemical potential control was performed on CHI 660A workstation (CHI, USA). All potentials were reported versus the Ag/AgCl (50 mM NaCl) reference electrode, which was calibrated as -72 mV vs. SCE.

2.3. DNA sample preparation

To maintain the constant ionic strength, preserve DNA physiological pH, and to avoid strand splitting effects or strong condensation, the pH 7.1 THB was used for DNA solution. The DNA samples for free adsorption were prepared by dropping a portion of 8 μ l DNA solutions onto a freshly cleaved HOPG, leaving it static for 30 min for the adsorption process to proceed. The residues of the solution were gently blown off, then rinsed with doubly distilled water to remove the remnants of the salts, and dried in the air before AFM imaging.

For DNA samples prepared by electrochemical deposition, a portion of 1 ml DNA solutions was placed in the electrochemical cell. A positive potential was applied to the HOPG electrode for 30 min for DNA deposition. The modified HOPG electrode was rinsed with doubly distilled water and dried in air ready for use.

2.4. Atomic force microscopy imaging

AFM images were recorded on a SPA 300HV (SEIKO Instruments, Chiba, Japan) in tapping mode at room temperature. Silicon Nanosensors I-shaped cantilevers of 225 μ m length and 15 Nm^{-1} spring constant were used. The radius of the silicon probe tip was about 20 nm. Typical imaging parameters used were: (1) work frequencies, 120–140 kHz; (2) work oscillation amplitude, 0.5–1.0 V; (3) scan rate, 0.5–1.0 Hz. Images were processed by flattening to remove the background slope, and the contrast and brightness were adjusted. All images were visualized using the Scanning Probe Image Processor, SPIwin (SPI3800, version 2.31F, copyright(C) 2001 SII). The height of the feature of interest was calculated by subtracting the background height in the area of featureless bare HOPG. The mean values of the heights were calculated using 30–60 measurements over different scanned images. The Origin (version 6.0 professional from Microcal Software, Inc., Northampton, MA) was used to calculate standard deviation (SD).

3. Results and discussion

3.1. DNA immobilization on HOPG by free adsorption

Due to their atomically flat surfaces, both HOPG and mica were usually used as the substrates for morphological studies [11–13]. Since mica has a hydrophilic surface, the interfacial tension helps the DNA molecules to spread over the surface and accelerates the adsorption process. However, HOPG has a hydrophobic surface; the interaction with DNA molecules is rather weak. A sufficient interval for the diffusion and adsorption of DNA on HOPG was determined as 30 min, which is required to form a well-defined morphology.

The HOPG electrode modified by CTDNA through free adsorption was obtained from different concentration of CTDNA solutions. The adsorption from 0.1 mgml^{-1} CTDNA solution showed that the DNA molecules adsorbed were self-organized into a very tight and well-spread two-dimensional network, as shown in Fig. 1(A). The DNA chains appear to cross-link together by randomly superimposing and overlapping. The height contour along the network was uniform, the average height over several regions was determined as 3.8 ± 0.2 nm. When the concentration was lowered to 0.05 mgml^{-1} , the surface coverage density decreased and the DNA film became less compact (Fig. 1(B)). The 3.5 ± 0.4 nm thickness of the film was observed. For the concentration of DNA was as low as 0.01 mgml^{-1} , certain amount of new DNA fragments at a height of 1.2 ± 0.2 nm appeared (Fig. 1(C)). Together with some thick DNA aggregation ropes of 4.6 ± 0.3 nm

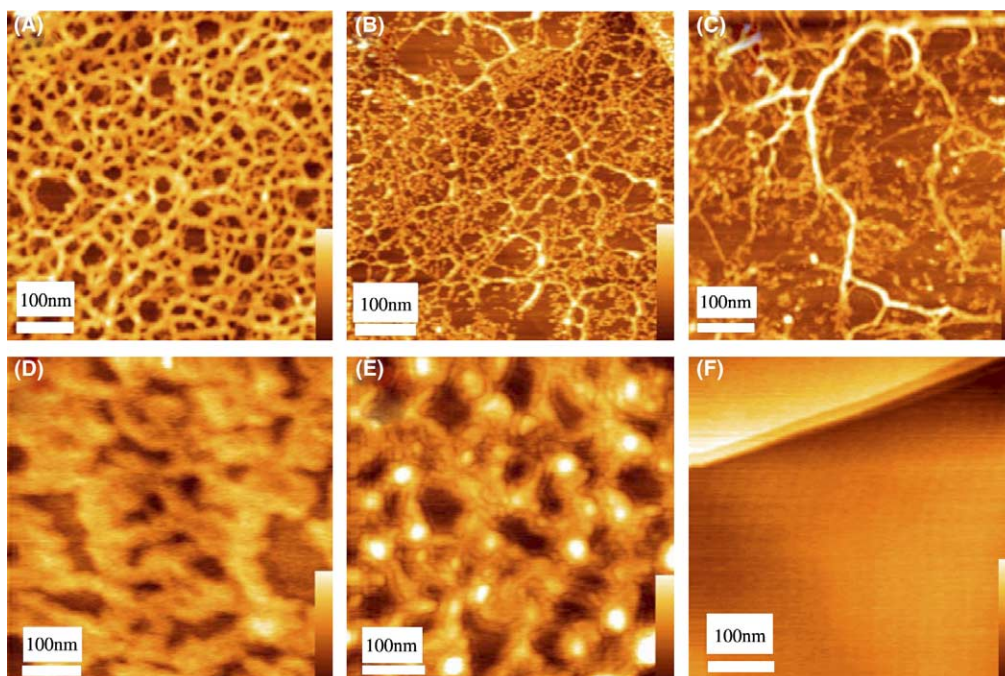


Fig. 1. Tapping mode AFM images of DNA on HOPG (A–C) prepared by 30 min of free adsorption from DNA/THB solutions: (A) 0.1 mg ml^{-1} CTDNA, (B) 0.05 mg ml^{-1} CTDNA, (C) 0.01 mg ml^{-1} CTDNA, (D) 0.01 mg ml^{-1} 20-bp oligo(dA)·oligo(dT), (E) 0.01 mg ml^{-1} 20-bp oligo(dG)·oligo(dC), and (F) no DNA. Height scale: (A) 6.4 nm, (B) 6.1 nm, (C) 7.3 nm (D) 1.7 nm, (E) 2.6 nm.

in height, two typical heights, 4.6 ± 0.3 and 1.2 ± 0.2 nm, were present.

As is well known, the most common physiological form of native DNA is the B form, while the DNA attached to HOPG is highly dehydrated and adopts the A-form with ca. 2.6 nm of double-helix diameter [14]. Since the finite probe tip radius of the AFM could lead to a width broadening of the molecule, the true representation of the DNA diameter should be given by the height measurements, which are little affected by variations in tip radius. The reported heights for double-helix DNA vary from 0.5–1.9 to 0.7 ± 0.2 nm for dsDNA freely adsorbed on HOPG [15]. The discrepancy between our measurements and the expected value is probably due to the DNA aggregation and the compression caused by the AFM tip. The height of 1.2 ± 0.2 nm for straight portions of CTDNA molecules should be associated with A-form DNA after a strong dehydration. The 3.8 ± 0.2 nm height assembled from 0.1 mg ml^{-1} CTDNA may be attributed to an aggregation and superposition of the DNA. It could be also observed that the DNA wire appeared in the network was bundled by several single DNA helices, which may be resulted from the mutual stabilization of neighboring chains under dehydrating conditions [11].

Recently, we found that oligonucleotides with a specific base sequence self-assembled reticulation structure on HOPG. The oligo(dA)·oligo(dT) assembled a cross-interlaced network on HOPG (Fig. 1(D)). The DNA chains cross-over together and the chain height was

0.8 ± 0.2 nm. However, oligo(dG)·oligo(dC) assembled a uniform reticulated structure with a height of 1.5 ± 0.2 nm (Fig. 1(E)). The difference in conformation for these synthetic dsDNA may be related to their diverse structure in solution. Since the oligo(dA)·oligo(dT) exhibits a typical B-form and resists to transform into other helical forms [14], it is not surprising that the oligo(dA)·oligo(dT) presents a typical B-form height of 0.8 nm. However, due to the self-association of oligo-(dG) strands [16], some triple-stranded segments would be presented in the oligo(dG)·oligo(dC) sample, which may result in the height of 1.5 nm seen in Fig. 1(E).

The 20 bp duplexes have a length only about 7 nm while their diameter is ca. 2 nm [18]. Thus, it seems impossible to form a network on solid substrates. However, during the DNA deposition on HOPG, the interaction of dsDNA with the HOPG substrate, the molecules overlap and superimpose, interacting through “sticky-ended” cohesions may occur, which could lead to conformation changes, DNA–DNA interactions, and formation of various network structure [18]. Certainly, the 20 bp oligomers on HOPG assembled network structures uniformly covered on the surface with mesh sizes of about 20–40 nm rather than sub-monolayers or densely packed monolayers, as shown in Fig. 1(D) and (E).

To distinguish DNA features from the HOPG features and obtain the real morphology of DNA, the HOPG was freshly split and scanned for the background image, as shown in Fig. 1(F). It shows a rather flat surface with expected occasional steps, which are the

characteristics of cleaved graphite surfaces. No topographic features appearing similar to those DNA structures were observed.

3.2. Mechanism of DNA free adsorption

It has been found that adenine, guanine, thymine and cytosine could condense into a monolayer film on graphite spontaneously [17]. The melting or separating of DNA strands would expose the hydrophobic bases to the solution. Thus, it is not surprising that a DNA molecule could adsorb freely onto graphite through the base–substrate interaction.

We have observed that the dsDNA may form intermediate cross-linkage points, and the density of the cross-linkage points was much higher on hydrophobic HOPG than on hydrophilic mica. Considering that when a dsDNA molecule adsorbed on HOPG, the hydrophobic core is exposed periodically, these hydrophobic spots would interact with the hydrophobic substrate, leading to the stabilization of the adsorption. On the other hand, the hydrophobic spots of dsDNA molecules could interact with each other when the strands crossing over or lying parallel, which may finally lead to the hybridization between the strands, forming cross-structures with specific height.

Since G–C base pairing through three hydrogen bonds and only two for A–T, the dissociation of A–T pair should be much easier than that of G–C pair. Certainly, oligo(dA)·oligo(dT) have stronger interaction with HOPG surface than oligo(dG)·oligo(dC). The

oligo(dA)·oligo(dT) chains tended to aggregate into a compact form instead of spreading over a distance. However, the oligo(dG)·oligo(dC) could spread over and form a lattice structure.

Free adsorption is a convenient way to form networks. However, some problems encountered with this approach include clumping of DNA into large unrecognized aggregates, and the DNA films were rather unstable and could be destroyed by the AFM scanning. This is due to the weakness of the physical interactions between the DNA molecules and the HOPG surface.

3.3. CTDNA immobilization on HOPG by electrochemical deposition

Gold surfaces modified with thiol-derivatized 15-mer oligo DNA duplexes have been investigated as a function of applied electrochemical potential via AFM [19]. But the densely packed DNA monolayer was not stable and could be desorbed from the surface at large positive potential, owing to the breakage of the gold-thiol linkages. In our work, the native CTDNA on HOPG prepared at various applied potentials ranged from +0.5 to +2.0 V has been studied by AFM and different morphologies have been shown in Fig. 2. At a low potential of +0.5 V (Fig. 2(A)), the individual chains were essentially randomly oriented on the electrode surface, similar to the case of free adsorption. The condensed layer could be observed with two typical heights: 1.7 ± 0.4 and 4.4 ± 0.3 nm. With increasing of the applied potential, the substrate became more positively charged,

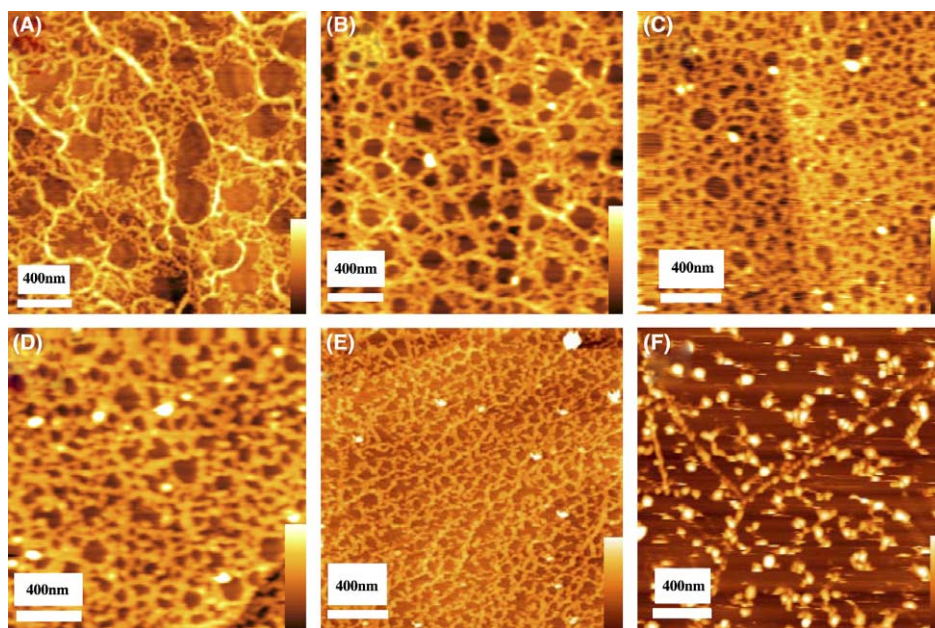


Fig. 2. Tapping mode AFM topographical images of the CTDNA modified HOPG surface prepared by 30 min of electrochemical deposition from a 0.1 mg ml^{-1} CTDNA/THB solution, at potentials: (A) +0.5, (B) +0.9, (C) +1.2, (D) +1.5, (E) +1.8, (F) +2.0 V (vs. 50 mM NaCl–Ag/AgCl). Height scale: (A) 8.1 nm, (B) 6.6 nm, (C) 6.2 nm, (D) 5.6 nm, (E) 10.0 nm, (F) 6.8 nm.

which could attract more CTDNA molecules to attach on it. The topological image of CTDNA at +0.9 V (Fig. 2(B)) indicates the density of CTDNA coverage increased and a well-defined lattice structure was formed. Some dark regions leaving the electrode surface exposed began to develop. The film also has two typical heights: 1.7 ± 0.3 nm and 2.8 ± 0.3 nm. For the potential of +1.2 V, the HOPG surface was covered uniformly by a compact CTDNA network, in which the DNA chains packed closely (Fig. 2(C)). The mesh size reduced in comparison with that for +0.9 V. The average thickness of the network was 2.1 ± 0.2 nm. For the potential of +1.5 V (Fig. 2(D)), a much thicker DNA intertexture was obtained with a uniform height of 2.5 ± 0.2 nm. The CTDNA chains were closely joined together and aggregated in end-to-end fashion. Fig. 2(E) showed a more compact DNA network formed under +1.8 V on HOPG. The mean thickness was 3.5 ± 0.3 nm and the mesh size was about 100 nm. Many bead-like nanoblocks appeared, periodically distributed along the strands, which was probably resulted from a close-stacking of the bases and superimposition of the double helix chains. Further increase of the potential to +2.0 V, we have observed abrupt changes in the DNA film (Fig. 2(F)). Large scale images revealed globular-like features of DNA layer appeared on the HOPG surface. The mean height of these DNA particles was 5.4 ± 0.3 nm. The high applied voltage may induce damage on the DNA and make its structure destroyed [20–22].

Although it has been reported that guanine is oxidized at ca. 1 V vs. SCE and adenine at ca. 1.2 V vs. SCE and the other bases may also be oxidized at even higher potentials, a potential less than 1 V vs. SCE is widely used for DNA deposition onto carbon electrodes [19–21]. However, the redox activity of DNA is strongly dependent on both the electrode material and the state of DNA. The bases in double-stranded native DNA with long chain (such as the native calf thymus double helix DNA of about 8 μm in length) are more electrochemically inactive than those in single-stranded DNA with short chains. Actually, no visual response was observed for the CTDNA at the HOPG electrode under

potentials up to 1.8 V (vs. 50 mM NaCl+Ag/AgCl), and significant responses happened at 2.0 V, at which the DNA chains were broken into fragments (Fig. 2(F)).

The effect of applied DC potentials on the state of deposited DNA and on the electrochemical sensing abilities is studied in our previous work [23], which demonstrated an optimal deposition potential of 1.8 V. We proposed that the DNA molecules could be polarized and aligned in the electric field and driven to attach to the HOPG surface via its one end forming an electrically conductive covalent-bonding linkages under this potential. It is possible that the formation of the networks is also a very important factor of stabilization of the bases, the densely packed electric conductive base-pair stacks could provide an integrated molecular orbital and behave as a huge macromolecule instead of individual bases.

The solution concentration still played a part in the DNA morphology though a potential of +1.8 V was applied on the HOPG electrode, which was demonstrated by the images in Fig. 3. Clearly, the DNA condensation became less compact and sparsely dendritic structures appeared with the decrease of the DNA concentration. The average heights were 3.1 ± 0.3 and 2.0 ± 0.2 nm for 0.05 mg ml^{-1} CTDNA (Fig. 3(B)) and 0.01 mg ml^{-1} CTDNA (Fig. 3(C)), which were less than that for 0.1 mg ml^{-1} CTDNA (Fig. 3(A)). Higher DNA concentration was better for obtaining a condensed deposition, while lower concentration was better for DNA chain extending and separating. The DNA chains interconnected and stretched linearly on the HOPG surface and were no longer uniformly smooth like that on mica.

The structure changes as a function of deposition time under a controlled potential of +0.5 V have also been investigated (Fig. 4). Obviously, the density of DNA condensation increased with time. At 30 s and 3 min, some cross-interlaced DNA fibers were observed (Fig. 4(A) and (B)). But many unrecognized aggregation parts appeared at 50 min (Fig. 4(C)). However, the film thickness did not change much and two typical heights around 2.0 and 4.5 nm were still present. This indicated that excess DNA molecules deposited during prolonged

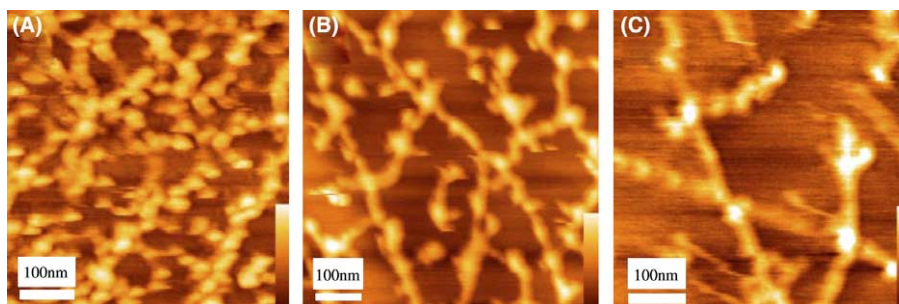


Fig. 3. Tapping mode AFM images of CTDNA on HOPG prepared by 30 min of electrochemical deposition at +1.8 V (vs. 50 mM NaCl–Ag/AgCl) from DNA/THB solutions: (A) 0.1 mg ml^{-1} , (B) 0.05 mg ml^{-1} , (C) 0.01 mg ml^{-1} . Height scale: (A) 5.5 nm, (B) 4.1 nm, (C) 3.3 nm.

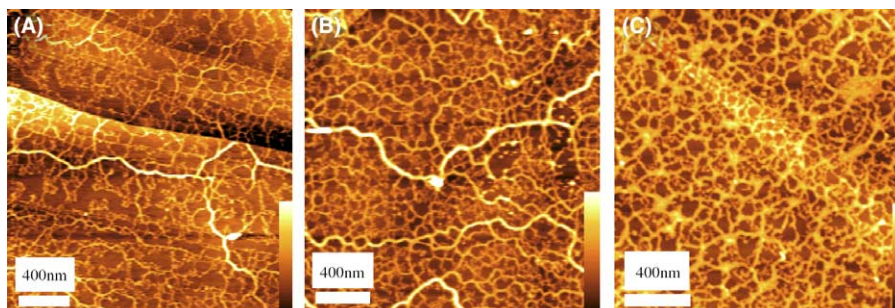


Fig. 4. Tapping mode AFM topographical images of the CTDNA modified HOPG surface prepared by electrochemical deposition at +0.5 V (vs. 50 mM NaCl–Ag/AgCl) from a 0.1 mg ml^{-1} CTDNA/THB solution, at intervals: (A) 30 s, (B) 3 min, (C) 50 min. Height scale: (A) 9.2 nm, (B) 9.8 nm, (C) 9.4 nm.

deposition period were favorably attached to the HOPG surface rather than to the deposited DNA layer.

In comparison with the free adsorption mentioned above, the formation and the molecular packing structure of the DNA film in the electrochemical environment could be controlled and modified in a flexible way by varying the applied potential on the substrate.

3.4. A possible mechanism of DNA electrochemical deposition

The applied positive DC potential generates a high electric field at the carbon–solution interface which extends only several nanometers depending on the concentration of the electrolyte [24]. However, due to the molecular conductivity the extended CTDNA long chain in the field of current flow would be polarized with one end with negative charge and another with positive charge [25]. The variations in morphology and thickness of DNA films indicate different modes of DNA condensation occurred at high and low potentials. In a low electric field, the DNA “rope” bundled by several chains cannot be undone due to the weak dipoles on every chain. It would condense on the HOPG surface along with the single chain, leaving the phosphate backbone to lie flat on the substrate. Such a DNA film was a thin layer with some thick “ropes”, which results two typical heights: 1.7 ± 0.4 and 4.4 ± 0.3 nm (Fig. 2(A)). As the applied potential increased, the induced dipoles on the chain would be reinforced. The thick “ropes” would be unwrapped to some extent. A uniform network could be obtained (Fig. 2(B)). Further increasing the potential, the polarization of DNA molecules was expected to be more strengthened, which made most of the DNA ropes undone. The extended DNA chain would be aligned and directed by the electrostatic forces. The positive electrode attracts the negative end and the negatively charged phosphate backbone, while pushes away the positive end of the chain. Therefore, the process of surface saturation on the electrode became much slower at high potential than at low potential.

It can be corroborated by the current–time curves during the DNA deposition, shown in Fig. 5. The deposition currents increased as the potential became more positive, from 0.5 to 1.8 V, while the time needed to approach a steady current became a little longer. Once the applied potential was withdrawn, the positive end of the chain would fall down on the substrate, and overlapping and superimposing of the DNA chains would occur, generating a more compact network as seen in Fig. 2(C)–(E).

The number of cross-linkages increased with the deposition potential rising from 1.2 to 1.8 V. This may be attributed to the increase of the film thickness. As the voltage increasing to 2.0 V, the induced dipoles of the DNA chain were strong enough to break the DNA chain into fragments, which may be oxidized at the electrode surface. The damages on the DNA structure could be seen in Fig. 2(F).

It is worth noting that, a variety of oxygen containing functional groups can be generated on the carbon electrode surface at high anodic potentials [26]. Some of these groups may bind covalently with the groups on the end of the DNA chain. This suggests that the electron transfer between the DNA and the electrode sur-

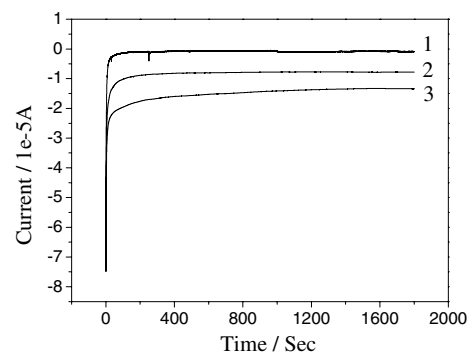


Fig. 5. Current–time dependence curve for DNA deposition on HOPG at: (1) 0.5 V, (2) 1.5 V and (3) 1.8 V, respectively. Other conditions are the same as in Fig. 2.

face would be accelerated. Certainly, a stable DNA film with excellent electrochemical properties could be obtained [23]. Further investigations are currently underway in our lab.

4. Conclusions

We have investigated both spontaneous condensation and potential-induced condensation of DNA molecules on HOPG by tapping mode AFM. Both native CTDNA and synthetic DNA could adsorb freely at the HOPG surface forming two-dimensional networks. The dsDNA molecules may form cross-linkage points on the chains. The morphological differences of the DNA adsorption demonstrate different interactions with the hydrophobic HOPG surface, which could be related to the differences in their intrinsic properties of base pairing. The effects of applied potential, DNA concentration and deposition time on the conformation of native CTDNA have been investigated. We have supposed that the DNA chain will become a macro-dipole in the electric field. The electrostatic force would align the macro-dipole, attracting its negatively charged end and the phosphate backbone to the electrode, and pushing the positively charged end away from the electrode. The electrostatic effect should be the dominant factor for the chain lying or standing on the substrate. Hence, it is conceivable to create preferred network structures of DNA layer by careful selection of the base composition and deposition procedure. The ability to modulate the morphology of a DNA film using small changes in potential may provide a unique design feature for the construction of biosensors and nano-scale electronic devices.

Acknowledgement

This work was supported by the Natural National Science Foundation of China (Grant No. 20075025).

References

- [1] A. Ullman, *An Introduction to Ultrathin Organic Films: From Langmuir–Blodgett to Self-Assembly*, Academic Press, Boston, 1991.
- [2] N.C. Seeman, *Nano Letters* 1 (2001) 22–26.
- [3] N.C. Seeman, *Curr. Opin. Struct. Biol.* 6 (1996) 519–526.
- [4] C.M. Niemeyer, *Appl. Phys. A* 68 (1999) 119–124.
- [5] N.C. Seeman, *Acc. Chem. Res.* 30 (1997) 357–363.
- [6] K.M. Millan, S.R. Mikkelsen, *Anal. Chem.* 65 (1993) 2317–2323.
- [7] K. Hashimoto, K. Ito, Y. Ishimori, *Anal. Chem.* 66 (1994) 3830–3833.
- [8] X.H. Xu, A.J. Bard, *J. Am. Chem. Soc.* 117 (1995) 2627–2631.
- [9] T. Herne, M.J. Tarlov, *J. Am. Chem. Soc.* 119 (1997) 8916–8920.
- [10] M.D. Purugganan, C.V. Kumar, N.J. Turro, J.K. Barton, *Science* 241 (1988) 1645–1649.
- [11] G. Lee, P.G. Arscott, V.A. Bloomfield, D.F. Evans, *Science* 244 (1989) 475–477.
- [12] P.G. Arscott, G. Lee, V.A. Bloomfield, D.F. Evans, *Nature* 339 (1989) 484–486.
- [13] S. Tanaka, Y. Naeda, L.T. Cai, H. Tabata, T. Kawai, *Jpn. J. Appl. Phys.* 40 (2001) 4217–4220.
- [14] W. Saenger, *Principles of nucleic acid structure*, in: Ch.R. Cantor (Ed.), *Springer Advanced Texts in Chemistry*, Springer-Verlag, New York, 1984.
- [15] H.G. Hansma, L. Revenko, K. Kim, D.E. Laney, *Nucleic Acids Res.* 24 (1996) 713–720.
- [16] M.A. Batalia, E. Protozanova, R.B. Macgregor, D.A. Erie, *Nano Letters* 2 (2002) 269–274.
- [17] N.J. Tao, Z.J. Shi, *Phys. Chem.* 98 (1994) 1464–1671.
- [18] N.C. Seeman, *Annu. Rev. Biophys. Biomol. Struct.* 27 (1998) 225–248.
- [19] Sh.O. Kelley, J.K. Barton, N.M. Jackson, Lee.D. Mcpherson, A.B. Potter, E.M. Spain, M.J. Allen, M.G. Hill, *Langmuir* 14 (1998) 6781–6784.
- [20] J. Wang, *Nucleic Acids Res.* 28 (2000) 3011–3016.
- [21] E. Paleček, M. Fojta, *Anal. Chem.* 73 (2001) 74A–83A.
- [22] E. Paleček, *Talanta* 56 (2002) 809–819.
- [23] X.Q. Lin, X.H. Jiang, L.P. Lu, *Biosensors and Bioelectronics*, in press.
- [24] A.J. Bard, L.R. Faulkner, *Electrochemical Methods: Fundamentals and Applications*, Wiley, New York, 1980 (Chapters 1 and 12).
- [25] D. Porschke, *Biophys. Chem.* 66 (1997) 241–257.
- [26] P.L. Runnels, J.D. Joseph, M.J. Logman, R.M. Wightman, *Anal. Chem.* 71 (1999) 2782–2789.